Distribution Pattern of Choroidal Thickness at the Posterior Pole in Chinese Children With Myopia

Junjie Deng,[1,2] Xiaoli Li,[3] Jiali Jin,[1] Bo Zhang,[1] Jianfeng Zhu,[1] Haidong Zou,[1,2] Xun Xu,[1,2] Jingbo Xie,[4] Ling Wang,[4] Shaopin Zhu,[1,2] and Xiangui He[1,4]

[1]Department of Preventative Ophthalmology, Shanghai Eye Diseases Prevention and Treatment Center, Shanghai Eye Hospital, Shanghai, China
[2]Department of Ophthalmology, Shanghai General Hospital, Shanghai Jiao Tong University, Shanghai Key Laboratory of Ocular Fundus Diseases, Shanghai Engineering Center for Visual Science and Photomedicine, Shanghai, China
[3]Wuhan University School of Health Sciences, Wuhan, China
[4]Department of Maternal and Child Health, School of Public Health, Key Laboratory of Public Health Safety, Ministry of Education, Fudan University, Shanghai, China

Correspondence: Xiangui He, Department of Preventative Ophthalmology, Shanghai Eye Diseases Prevention and Treatment Center, Shanghai Eye Hospital, No. 380 Kangding Road, Shanghai 200040, China;
xianhezi@163.com.
Shaopin Zhu, Department of Preventative Ophthalmology, Shanghai Eye Diseases Prevention and Treatment Center, Shanghai Eye Hospital, No. 380 Kangding Road, Shanghai 200040, China;
zhushaopinbaby@126.com.

JD and XL contributed equally to the work presented here and should therefore be considered equivalent authors.

Submitted: August 3, 2017
Accepted: February 21, 2018

Citation: Deng J, Li X, Jin J, et al. Distribution pattern of choroidal thickness at the posterior pole in Chinese children with myopia. *Invest Ophthalmol Vis Sci*. 2018;59:1577–1586. https://doi.org/10.1167/iovs.17-22748

Purpose. To determine the relationship between choroidal thickness (ChT) at the posterior pole and refractive error and to explore the difference between the macular and peripapillary regions in children with myopia.

Methods. A total of 340 healthy Chinese children underwent a series of comprehensive ocular examinations including cycloplegic refraction. Swept-source optical coherence tomography was used to measure the ChT in the macular and peripapillary regions. The Early Treatment of Diabetic Retinopathy Study grid was applied to define the sectors.

Results. The mean spherical equivalent (SE) of the participants was −1.71 ± 2.22 diopter (D; range from −7.63 to 4.25 D). The mean ChT in the central foveal, parafoveal, and perifoveal regions were 229 ± 65 μm, 227 ± 60 μm, and 215 ± 50 μm, respectively, and the mean global peripapillary choroidal thickness (PPCT) was 136 ± 33 μm. The choroid in the macular region and the global PPCT was thinner in myopes compared to hyperopes. The area between the central fovea and the optic disc underwent the largest change as myopia worsened. SE, uncorrected visual acuity, cornea curvature radius (CR), retinal thickness (RT), and retinal nerve fiber layer thickness (RNFLT, except for the central fovea) were the independent factors of ChT in the macular region. SE, CR, RT, and RNFLT were the independent factors of PPCT temporally, inferiorly, and globally, while only CR, RT, and RNFLT were independently associated with PPCT superiorly and nasally.

Conclusions. Choroidal thinning might be uneven during the development of myopia. SE only influenced the macular area and sectors temporal and inferior to the optic disc.

Keywords: children, choroid, myopia, refractive error, optical coherence tomography

The prevalence of myopia is increasing in Chinese children. Choroidal thinning and atrophy are important pathological changes during the development of myopia. Choroidal atrophy can lead to dysfunction or atrophy of the outer retina and cause visual impairment. The choroid has also been reported to play an important role in the development of refractive error in animal models.[1–3]

Recent advancements in optical coherence tomography (OCT) technology have provided us with opportunities to observe the choroid in vivo and measure choroidal thickness (ChT), which was considered to be useful in grading myopic fundus changes. Among OCT technologies, enhanced depth imaging optical coherence tomography (EDI-OCT) and swept-source optical coherence tomography (SS-OCT) are commonly used to study ChT.[4,5]

Following these technological advances, an increasing number of studies have investigated ChT in healthy children, and have mainly focused on ChT in the macular region, as the choroid in the macular region is of great importance to supply oxygen and nutrients to the retina in the central foveal area, an area that is important to visual acuity.[6–16] Studies of the macular region in pediatric populations have indicated a thinning of the choroid was associated with increased degree of myopia and axial length (AL),[8,12,14,15] which is similar to results obtained from adults.[5,17,18] However, with regard to age, past studies carried out in adults have indicated a reduction in ChT with increasing age,[5,17–19] but the results from pediatric populations have not been uniform.[6–8,10–16] The exact reason for such difference between children and adults is still unclear, probably due to the growth and development of eyeball during childhood.

Compared to the number of studies focusing on the ChT in the macular region, fewer studies have investigated the link between ChT and refractive error in the peripapillary region in

pediatric populations. In adults, ChT in the peripapillary region (also called PPCT) has been found to be thinner in those high myopes compared to emmetropes,[20] while in myopic children, the global PPCT was not significantly thinner than that of nonmyopic children.[21,22] The mechanisms that lead to such discrepancy are still unclear. Although the global PPCT was not significantly thinner in myopic children than that of nonmyopic children, the PPCTs in some sectors achieved significance. However, the results from these limited studies were also inconsistent with each other.[21,22]

The limited number of studies of PPCT in pediatric populations, small sample sizes, and unclear influencing factors mean that ChT warrants further study with a larger sample size. Moreover, no study has reported ChT in a wide area of the posterior pole in both the macular and peripapillary regions in the same healthy pediatric population with different refractive statuses. Hence, the aim of the current study was to determine whether ChT in the macular and peripapillary regions is associated with refractive error in Chinese children and whether such association is similar in both the two regions.

Methods

Settings and Participants

This cross-sectional study was conducted during May 2016 at a single school in the Baoshan district in Shanghai, China. Healthy Chinese children aged between 9 and 16 years with different refractive status were included in the study. Children with ptosis, amblyopia (best corrected visual acuity < 20/25), strabismus, congenital cataracts or glaucoma, fundus diseases, or previous ocular surgeries were excluded from the study.

Ethical approval for this study was obtained from the Institutional Review Board of Shanghai General Hospital, Shanghai Jiao Tong University, and the study was performed in accordance with the tenets of the Declaration of Helsinki. All participating children as well as their parents or guardians received a detailed explanation of the study protocol. Written informed consent was obtained from the parents or guardians before the study, and oral consent was obtained from the participating children.

The examination team was composed of one ophthalmologist, two public health physicians, five optometrists, and two nurses, and all examinations followed the approved protocol. The height and weight of all participants were measured at the beginning of the study.

Ocular Examinations

The children underwent a series of comprehensive ocular examinations to measure visual acuity, AL, intraocular pressure (IOP), slit-lamp examination, cycloplegic refraction, and OCT examination. Visual acuity was tested at a 4-meter distance using a retro-illuminated Early Treatment of Diabetic Retinopathy Study (ETDRS) chart. Children who wore spectacles were asked to undergo the visual acuity assessment with and without spectacles, respectively. AL was obtained by ocular biometry (IOL Master, version 5.02, Carl Zeiss Meditec, Oberkochen, Germany), and IOP was obtained using a noncontact tonometer (model NT-4000, Nidek, Inc., Fremont, CA, USA). Refraction and corneal curvature measurements were acquired using an autorefractor, after cycloplegia was accomplished (KR-8900, Topcon, Tokyo, Japan). The detailed protocol for cycloplegia was as follows: children received one drop of 0.5% proparacaine (Alcaine; Alcon, Fort Worth, TX, USA) in each eye, followed by two drops of 1% cyclopentolate (Cyclogyl; Alcon), with each drop 5 minutes apart. The absence of a light reflex and pupil size larger than 6 mm were deemed to indicate the presence of cycloplegia, and this was examined at least 30 minutes after the last drop of cyclopentolate was administered. The children were asked to undergo subjective refraction after cycloplegia examinations if their presenting visual acuity was less than 20/25.

ChT Measurements

SS-OCT (DRI OCT-1 Atlantis, Topcon) was used to measure ChT in both the macular and peripapillary regions of the right eyes. Children whose OCT images were clear and with image signal strength larger than 60 in both the macular and peripapillary regions were included in the final analyses. The SS-OCT parameters were as follows: wavelength of the SS-OCT light source = 1050 nm, scan rate = 100,000 A-scans per second, depth of the scan window = 2.6 mm, axial resolution = 8 μm, and transverse resolution = 10 μm. The SS-OCT examinations were performed (after cycloplegia was induced) by one trained examiner from 10:00 AM to 3:00 PM each day to minimize the influence of diurnal variation.[23] Diopter (D) of spherical power, cylindrical power, AL and cornea curvature radius (CR) were input into the OCT system to compensate for the magnification factors associated with AL before each OCT image collection. Each SS-OCT examination included 12 radial OCT scan lines focused on the center of the fovea or the optic disc, which correspond to macular and peripapillary measurements, respectively. Each scan line was 12 mm long and separated from the adjacent lines by 15°. Thirty-two B-scan OCT images were obtained on each scan line, and were automatically averaged by built-in software to create an averaged image. Segmentation of different layers on the OCT images and construction of topographic maps were automatically completed by built-in software. The segmentation was carefully inspected and confirmed by one OCT technician who was masked to the refractive status of the participants, and manual correction was performed when the software misjudged the borderline of each layer. Segmentation was manually corrected in 82 participants (24.1%). In order to test the repeatability of manual correction, the first 20 images needed manual segmentation was manually corrected twice by the OCT technician. The mean difference between the first and second time manual correction was smallest in the inferior sector of the parafoveal region ([–0.55 ± 5.01] μm, 95% limits of agreement: –10.37∼9.27 μm) and was largest in the nasal sector of the parafoveal region ([3 ± 5.66] μm, 95% limits of agreement: –8.09∼14.09 μm). The correlation coefficient between the two manual corrections in each sector ranged from 0.991 to 0.999 (all $P < 0.001$). Considering the averaged thickness of the choroid, the difference between the first and second manual correction was acceptable and the repeatability of manual correction was good.

ChT was defined as the vertical distance between Bruch's membrane and the choroidal-scleral interface (Figs. 1A, 1C). The ETDRS grid was applied in the final analysis of ChT, and the averaged ChT in each sector of the grid was calculated by built-in software. The diameters for the inner circle (central foveal circle), middle circle (parafoveal circle), and outer circle (perifoveal circle) of the ETDRS grid were 1, 3, and 6 mm, respectively, and the inner ring (the area between the inner circle and the middle circle, also called the parafoveal region when it is located in the macular area) as well as the outer ring (the area between the middle circle and the outer circle, also called the perifoveal region when it is located in the macular area) were further divided into four quadrants, namely, the temporal, superior, nasal, and inferior quadrants. In the macular region, all nine sectors of the grid were applied (Fig.

Investigative Ophthalmology & Visual Science

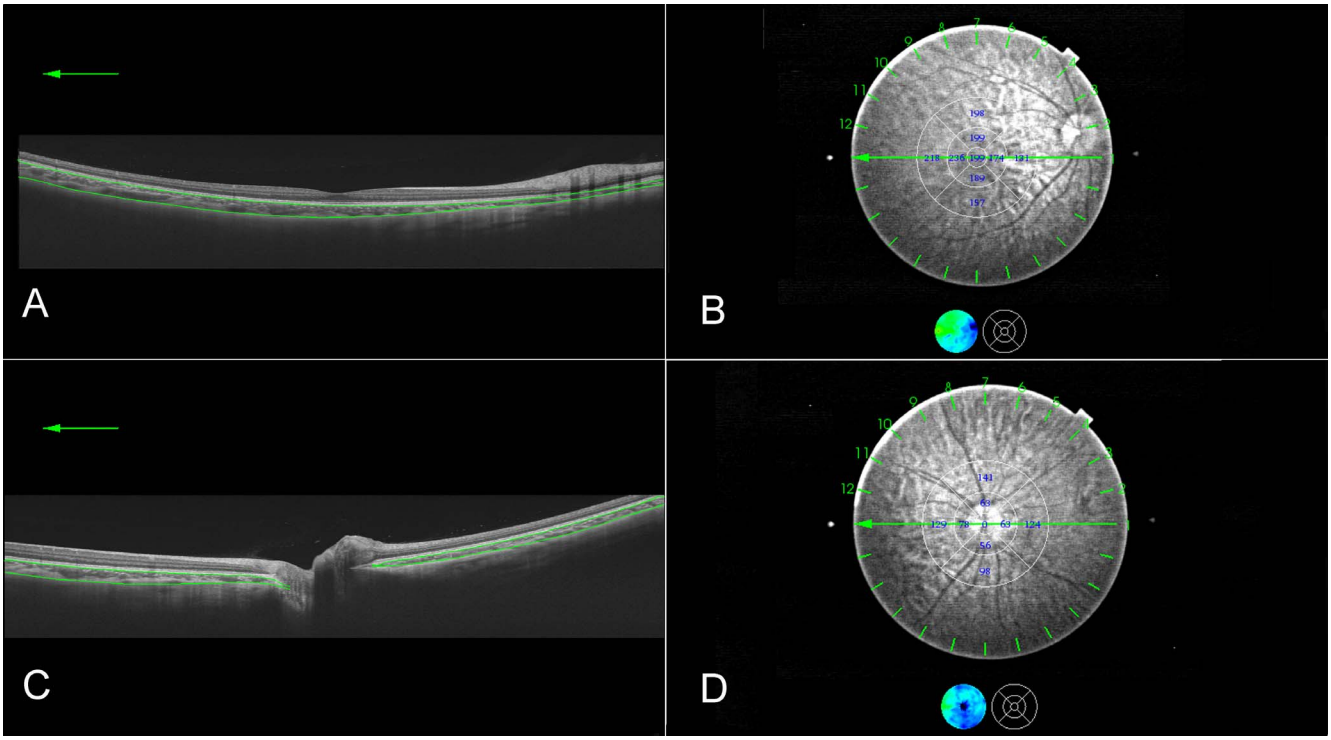

Figure 1. ChT maps of the same participant obtained by SS-OCT in both the macular region and the peripapillary region. (**A**) ChT measurement in the macular region. The ChT was defined as the vertical distance between Bruch's membrane (*upper green line*) and the choroidal-scleral interface (*lower green line*). (**B**) ETDRS grid of the macular region. The mean ChT (μm) of each sector is shown in the grid. (**C**) ChT measurement in the peripapillary region. The ChT was defined as the vertical distance between Bruch's membrane (*upper green line*) and the choroidal-scleral interface (*lower green line*). (**D**) ETDRS grid of the peripapillary region. The mean ChT of each sector is shown in the grid. As the inner circle and inner ring were affected by the optic disc and the measurements done by the software were not reliable, only measurements from the outer ring were used.

1B). In the peripapillary region, only four sectors in the outer ring were used in the final analysis because neither the inner circle nor the inner part of the inner ring contains choroidal tissue and the topographic maps in these sectors were not reliable (Fig. 1D). In addition, retinal thickness (RT) was defined as the vertical distance between the internal limiting membrane (ILM) and the retinal pigment epithelium, and retinal nerve fiber layer thickness (RNFLT) was defined as the vertical distance between the ILM and the interface between the retinal nerve fiber layer and the retinal ganglion cell layer. Both the RT and RNFLT were calculated automatically by the built-in software within the ETDRS grid.

Statistical Analysis

An online database system for real-time examination data input with logic automatically checked was used for data input in field work. Data of auto-refraction and ChT were uploaded from the instruments to the system directly. The output data set from the system for analysis were adjudicated by a staff to ensure that there were no discrepancies. Statistical software (IBM SPSS Statistics, Inc., Version 22.0, Chicago, IL, USA) was used to perform statistical analyses. Only data from the right eyes were included in the final analyses.

The data distribution was examined using the Kolmogorov-Smirnov test. Intergroup differences were assessed with *t*-tests or analysis of variance when the data were normally distributed and with the Mann-Whitney *U* test or Kruskal-Wallis test when the data were abnormally distributed. Three main analyses were performed. First, we compared mean ChT within the macular region and within the peripapillary region using analyses of variance and the Bonferroni method for post hoc tests. Second, we compared ChT in these regions according to refractive status (hyperopia, emmetropia, and myopia). Spherical equivalent (SE) (SE = sphere + 0.5*cylinder) was used to categorize these refractive statuses. Hyperopia, emmetropia, and myopia were defined as SE $\geq$ +0.5 D, −0.5 D < SE < +0.5 D, and SE $\leq$ −0.5 D, respectively. Additionally, mild myopia, moderate myopia, and high myopia were defined as −3.0 D < SE $\leq$ −0.5 D, −5.0 D < SE $\leq$ −3.0 D, and SE $\leq$ −5.0 D, respectively. Third, we identified the independent factors associated with ChT in different regions using stepwise multiple regression analysis and Variance Inflation Factor (VIF) values were used to considerate collinearity among parameters. In general, VIF < 10 indicates no multicollinearity among parameters. Weight, height, age, uncorrected visual acuity (UVA), IOP, SE, CR, RNFLT, and RT were included in the stepwise regression analysis. Statistical significance was defined as $P < 0.05$ (two-tailed).

Results

General Characteristics of the Study Participants

A total of 340 children (boys, $n = 170$; girls, $n = 170$) with a mean age of 11.93 ± 1.78 years (range from 9 to 16) were included. The mean SE, CR, and AL were −1.71 ± 2.22 D, 7.87 ± 0.26 mm, and 24.32 ± 1.16 mm, respectively. The mean SE for the myopic, emmetropic, and hyperopic group was −2.96 ± 1.67 D, 0.05 ± 0.24 D, and 1.04 ± 0.61 D, respectively. Detailed information is shown in Table 1. The mean age of myopes was 12.37 ± 1.80 years, older than the emmetropes (11.45 ± 1.53 years, $P = 0.001$) and hyperopes (10.87 ± 1.32 years, $P < 0.001$), while no difference between the emme-

Table 1. General Characteristic of Children

$N = 340$	Mean ± SD	Median	Min	Max
Systemic/ocular parameters				
Weight, kg	44.48 ± 14.05	43.10	21.90	99.50
Height, cm	150.21 ± 11.7	148.95	125.90	179.90
Age, y	11.93 ± 1.78	12.00	9.00	16.00
UVA	0.6 ± 0.39	0.50	0.04	2.00
SE, D	−1.71 ± 2.22	−1.50	−7.63	4.25
CR, mm	7.87 ± 0.26	7.89	6.91	8.64
AL, mm	24.32 ± 1.16	24.25	20.68	27.61
IOP, mm Hg	15.8 ± 2.52	16.00	10.00	24.00
BMI, kg/m^2	19.31 ± 3.96	18.71	12.05	35.24
ChT in the macular region, μm				
T1	245 ± 63	239	79	457
N1	201 ± 60	196	7	402
I1	233 ± 66	231	35	430
S1	229 ± 61	226	57	449
T2	249 ± 58	245	89	467
N2	160 ± 50	152	53	313
I2	223 ± 59	219	81	429
S2	228 ± 52	224	100	421
Central foveal ChT	229 ± 65	226	20	453
Parafoveal ChT	227 ± 60	222	48	428
Perifoveal ChT	215 ± 50	213	94	384
PPCT, μm				
T2	151 ± 45	148	49	297
N2	129 ± 41	125	42	243
I2	112 ± 35	108	46	255
S2	152 ± 40	151	71	272
Global PPCT	136 ± 33	136	61	234

One-way analysis of variance was used to compare the ChT in the central foveal region, parafoveal region, and perifovea region, and Bonferroni method was used for post hoc tests. Repeated measures analyses of variance and the Bonferroni method for post hoc tests were used for vertical and horizontal comparisons. Horizontal comparisons mean to compare the regions along the horizontal axis passing through the central fovea, including the temporal perifoveal sector, temporal parafoveal sector, central foveal region, nasal parafoveal sector, and nasal perifoveal sector. Vertical comparisons mean to compare the regions along the vertical axis passing through the central fovea, including the superior perifoveal sector, superior parafoveal sector, central foveal region, inferior parafoveal sector, and inferior perifoveal sector. BMI, body mass index; T1, temporal sector of inner ring; N1, nasal sector of inner ring; I1, inferior sector of inner ring; S1, superior sector of inner ring; T2, temporal sector of outer ring; N2, nasal sector of outer ring; I2, inferior sector of outer ring; S2, superior sector of outer ring.

tropes and the hyperopes ($P > 0.05$). The distribution of genders was not significantly different in different refractive groups.

ChT Is Greatest in the Central Foveal Region and Temporal Sectors in the Macular Region

The mean ChT in the central foveal region (229 ± 65 μm) was thicker than that in the parafoveal region (227 ± 60 μm) ($P = 0.001$), and the mean ChT in the parafoveal region was also thicker than that in the perifoveal region (215 ± 50 μm) ($P < 0.001$) (Table 1). The mean ChT decreased from the temporal perifoveal sector to the nasal perifoveal sector horizontally (all, $P < 0.05$). The mean ChT in the inferior perifoveal sector (223 ± 59 μm) was thinner than that of the central foveal region (229 ± 65 μm) ($P = 0.003$) and the inferior parafoveal region (233 ± 66 μm) ($P < 0.001$), while no significant difference was observed among the other sectors in the vertical direction (Table 1).

ChT Is Greatest in the Temporal and Superior Sectors in the Peripapillary Region

The mean global PPCT, which combined the mean PPCT of the four peripapillary sectors, was 136 ± 33 μm. The mean PPCTs in the temporal sector (151 ± 45 μm) and the superior sector (152 ± 40 μm) were thicker than those in the nasal sector (129 ± 41 μm) and the inferior sector (112 ± 35 μm) (all, $P < 0.001$), and the mean PPCT in the nasal sector was also thicker than that in the inferior sector ($P < 0.001$), while no difference was observed between the temporal sector and the superior sector. In addition, the mean PPCT in the four peripapillary sectors were thinner than ChT in all nine macular sectors. The detailed values for ChT in each sector are shown in Table 1.

Thinning of the Choroid in the Macular Region Is More Pronounced Than in the Peripapillary Region With the Increase of Degree of Myopia

The choroid in the central foveal region was thickest in the hyperopes (284 ± 55 μm), followed by the emmetropes (250 ± 66 μm), and was thinnest in the myopes (208 ± 57 μm) (Table 2). Similar findings were observed in the parafoveal region and the perifoveal region (all, $P < 0.05$). The ChT was 27%, 24%, and 22% smaller in the central foveal, parafoveal, and perifoveal regions, respectively, in myopes compared to hyperopes. The macular ChTs of all nine sectors were thinner in myopes compared to emmetropes (all, $P < 0.05$), and similar results were observed when comparing emmetropes with hyperopes, except for the two sectors in the inferior macular region. The relative difference in the ChT was most notable in the nasal sector and least notable in the superior sector in both the parafoveal and perifoveal regions when comparing myopes to hyperopes (Fig. 2A).

For the three subgroups of myopia, the ChT of the mild myopes (225 ± 53 μm) was greater than that of both the moderate myopes (191 ± 52 μm) and the high myopes (182 ± 61 μm) in all nine sectors of the macular region, as well as in the parafoveal and perifoveal regions (all, $P < 0.05$). However, no differences in ChT were observed between the moderate myopes and the high myopes in any sectors of the macular region (Table 3). The ChT was 19%, 17%, and 15% smaller in the central foveal, parafoveal, and perifoveal regions, respectively, in high myopes compared to mild myopes. The relative difference of ChT was most notable in the nasal sector in both the parafoveal and perifoveal region when comparing high myopes to mild myopes (Fig 2B).

In the peripapillary region, the mean global PPCT of the hyperopes (151 ± 34 μm) was thicker than that of the emmetropes (137 ± 34 μm, 9% thinner) and the myopes (131 ± 31 μm, 13% thinner) (both, $P < 0.05$), while no difference was observed in the PPCT between the myopes and the emmetropes (Table 2). Unlike the global PPCT, the PPCT in the temporal sector was greater in the hyperopes (183 ± 42 μm) than that of the emmetropes (157 ± 45 μm), and the PPCT in the temporal sector was also greater in the emmetropes than that in the myopes (139 ± 41 μm) (both, $P < 0.05$), which was similar to the changing pattern in the macular region. In the temporal sector, PPCT was 24% smaller in myopes compared to hyperopes ($P < 0.05$), which was also similar to the macular region. In the inferior and superior sectors, PPCT was 20% ($P < 0.05$) and 8% smaller, respectively, in myopes compared to hyperopes, although it did not reach statistical significance in the superior sector (Fig. 2A). However, in the nasal sector, no difference was observed among the three groups. Moreover, no difference was observed among the three myopic subgroups in all four sectors or globally (Table 3), although the PPCT of the

Investigative Ophthalmology & Visual Science

Table 2. Comparison of ChTs in Children With Different Refractive Statuses in the Macular and Peripapillary Regions

	Myopes, $N = 222$	Emmetropes, $N = 49$	Hyperopes, $N = 69$	Total, $N = 340$	*P* Value
ChT in the macular region, μm					
T1	225 ± 53	265 ± 64	295 ± 57	245 ± 63	<0.001*
N1	181 ± 51	222 ± 62	250 ± 52	201 ± 60	<0.001†
I1	213 ± 58	259 ± 68	280 ± 59	233 ± 66	<0.001†
S1	210 ± 54	247 ± 60	273 ± 55	229 ± 61	<0.001†
T2	232 ± 50	269 ± 56	290 ± 59	249 ± 58	<0.001†
N2	143 ± 43	175 ± 47	202 ± 47	160 ± 50	<0.001*
I2	205 ± 52	248 ± 61	263 ± 54	223 ± 59	<0.001†
S2	214 ± 48	242 ± 49	262 ± 50	228 ± 52	<0.001*
Central foveal ChT	208 ± 57	250 ± 66	284 ± 55	229 ± 65	<0.001†
Parafoveal ChT	207 ± 52	248 ± 60	275 ± 52	227 ± 60	<0.001†
Perifoveal ChT	199 ± 43	233 ± 48	254 ± 46	215 ± 50	<0.001*
PPCT, μm					
T2	139 ± 41	157 ± 45	183 ± 42	151 ± 45	<0.001†
N2	131 ± 39	127 ± 44	125 ± 41	129 ± 41	0.521†
I2	105 ± 32	115 ± 37	132 ± 37	112 ± 35	<0.001*
S2	149 ± 40	151 ± 40	163 ± 39	152 ± 40	0.052†
Global PPCT	131 ± 31	137 ± 34	151 ± 34	136 ± 33	<0.001†

T1, temporal sector of inner ring; N1, nasal sector of inner ring; I1, inferior sector of inner ring; S1, superior sector of inner ring; T2, temporal sector of outer ring; N2, nasal sector of outer ring; I2, inferior sector of outer ring; S2, superior sector of outer ring.

* Statistical significance was tested using the Kruskal-Wallis test.

† Statistical significance was tested using analysis of variance.

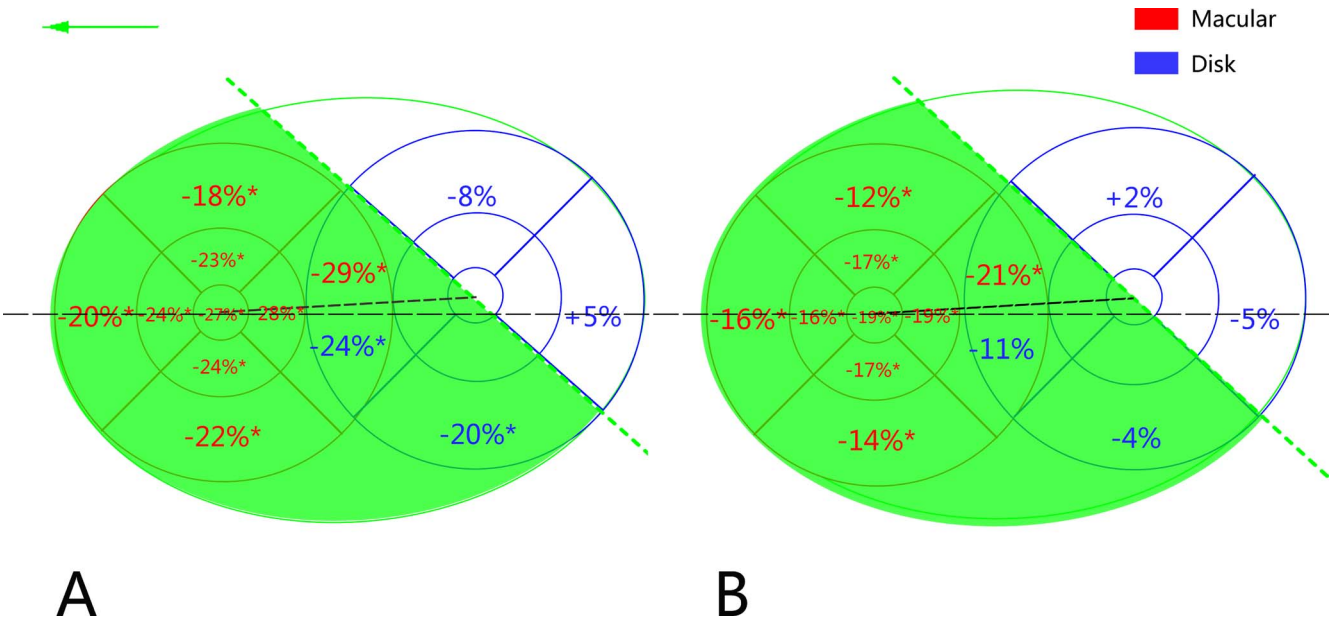

Figure 2. Relative difference in the ChT in different regions of the posterior pole. (**A**) The *red* ETDRS grid shows the relative difference in ChT in the macular region between the hyperopia and myopia group, and the *blue* ETDRS grid shows the relative difference in ChT in the peripapillary region between the hyperopia and myopia group. The *green oval circle* represents the posterior pole explored in the current research. The *long dash line* shows the horizontal line of the whole fundus and the *short dash line* shows the connecting line of foveal center and disc center. As shown in the image, the area between the central fovea and the optic disc has the largest difference. The *green-colored sectors* show the area affected by SE, where the ChT decreased with the increase in the degree of myopia. Significant comparisons are marked by *asterisks* (*). (**B**) The *red* ETDRS grid shows the relative difference in ChT in the macular region between the mild myopia and high myopia group, and the *blue* ETDRS grid shows the relative difference in ChT in the peripapillary region between the mild myopia and high myopia group. The *long dash line* shows the horizontal line of the whole fundus and the *short dash line* shows the connecting line of foveal center and disc center. As shown in the image, the area between the central fovea and the optic disc also has the largest difference. The *green-colored sectors* show the area affected by SE, where the ChT decreased with the increase in the degree of myopia. Significant comparisons are marked by *asterisks* (*).

Investigative Ophthalmology & Visual Science

Table 3. Comparison of ChTs in Children With Different Myopic Levels in the Macular and Peripapillary Regions

	Mild Myopes, $N = 119$	Moderate Myopes, $N = 72$	High Myopes, $N = 31$	*P* Value
ChT in the macular region, μm				
T1	242 ± 51	207 ± 49	204 ± 53	<0.001*
N1	196 ± 48	166 ± 47	158 ± 57	<0.001*
I1	229 ± 55	195 ± 56	191 ± 56	<0.001*
S1	225 ± 53	196 ± 48	187 ± 56	<0.001*
T2	247 ± 48	217 ± 48	209 ± 40	<0.001*
N2	155 ± 42	132 ± 38	123 ± 45	<0.001†
I2	217 ± 50	193 ± 53	186 ± 43	0.001*
S2	226 ± 49	203 ± 44	198 ± 39	0.001*
Central foveal ChT	225 ± 53	191 ± 52	182 ± 61	<0.001*
Parafoveal ChT	223 ± 48	191 ± 48	185 ± 54	<0.001†
Perifoveal ChT	211 ± 42	186 ± 41	179 ± 37	<0.001*
PPCT, μm				
T2	144 ± 39	137 ± 40	128 ± 47	0.127*
N2	133 ± 40	131 ± 41	126 ± 37	0.721†
I2	107 ± 30	104 ± 34	102 ± 37	0.492†
S2	149 ± 35	148 ± 44	153 ± 47	0.870*
Global PPCT	133 ± 29	130 ± 32	127 ± 35	0.599*

T1, temporal sector of inner ring; N1, nasal sector of inner ring; I1, inferior sector of inner ring; S1, superior sector of inner ring; T2, temporal sector of outer ring; N2, nasal sector of outer ring; I2, inferior sector of outer ring; S2, superior sector of outer ring.

* Statistical significance was tested using analysis of variance.

† Statistical significance was tested using the Kruskal-Wallis test.

temporal sector was 11% smaller in high myopes (128 ± 47 μm) compared to mild myopes (144 ± 39 μm) (Fig. 2B).

Independent Factors Associated With ChT

Table 4 shows the independent factors of ChT in different regions. In the central foveal region, SE, UVA, CR, and RT were significantly and independently associated with ChT. Similarly, SE, UVA, CR, RT, and RNFLT were independently associated with ChT in the parafoveal and perifoveal regions. However, age was not significantly associated with ChT as an independent factor in the regression models (central foveal region: $\beta = -0.026$, $P = 0.628$; parafoveal region: $\beta = 0.003$, $P = 0.955$; perifoveal region: $\beta = 0.030$, $P = 0.570$). Every 1 D increase in the degree of myopia was associated with 14.4-, 11.2-, and 8.0-μm decreases in the mean ChT in the central foveal, parafoveal, and perifoveal regions, respectively. The overall R^2 of the three models were 0.325, 0.355, and 0.318, respectively.

In the peripapillary region, SE, CR, RT, and RNFLT were independently associated with the global PPCT as well as PPCTs in the temporal sector and the inferior sector, while in the superior sector and the nasal sector, the independent factors were only CR, RT, and RNFLT. Every 1 D increase in the degree of myopia was associated with 3.2-, 5.5-, and 4.3-μm decreases in the global, temporal, and inferior PPCTs, respectively.

Taken together, these results indicate that the ChTs in the macular region and the PPCTs in the temporal and inferior sectors decrease as the degree of myopia increases, while the PPCTs in the superior and nasal sectors remain relatively constant (Figs. 2A, 2B).

Discussion

To our knowledge, this study is the first to simultaneously explore ChTs in both the macular region and peripapillary region in a pediatric population. The current results indicate that the choroid in the macular region became thinner when the SE became myopic-shifted. This trend was more obvious in the central foveal region compared with the parafoveal and perifoveal regions. However, in the peripapillary region, only the temporal and the inferior sectors thinned as the refractive status shifted from hyperopia to myopia, and in general the percentage differences (24% temporal and 20% inferior) were smaller compared with that of the macular region (from 18% to 29% in all sectors). Choroidal thinning was most evident in the area between the central fovea and the optic disc. Multiple regression analysis showed that SE was an independent factor of the macular region and the area temporal and inferior to the optic disc, not the area superior and nasal to the optic disc.

Varied ChT at the Posterior Pole

The mean ChT observed in our study (229 ± 65 μm in the central foveal region) was smaller than those reported by previous studies (251∼337 μm in the central foveal region).[8,12,14] The choroid in the macular region was thickest in the temporal sector and thinnest in the nasal sector, which was similar to that in previous studies carried out in pediatric populations.[7,8,10–13,15] The mean global PPCT in our study (136 ± 33 μm) was also smaller than the mean PPCTs reported by a previous study (165 ± 34 μm).[22] Age, race, refractive status as well as the instruments and protocols used may contribute to these differences. In our study, the mean PPCT was measured automatically by built-in software, and the area included in the study was 1.5 to 3.0 mm away from the center of the optic disc. As more positions were measured automatically, our results could reflect a more accurate PPCT in a Chinese pediatric population.

As the number of studies performed in the peripapillary region in the pediatric population is small, the regional distribution of the PPCT in children is still unclear. We found that the PPCT was thinnest in the inferior sector, which reflects results found in studies with both children and adults.[21,22,24–26] This consistent finding may be due to the developmental pattern of the eyes, as the optic fissure is located inferiorly and is the last part to close during ocular development.[27] With regard to the temporal and superior sectors, we found there to be a thicker choroid in temporal and superior sectors compared to the nasal and inferior sectors, and no difference in thickness between the temporal and superior sectors. Some previous studies carried out in both adults and children have reported the thickest PPCT to be in the superior sector,[22,24–26,28] while others found the thickest PPCT in the temporal sector.[29] A thick choroid in the temporal sector may be the result of higher demand for oxygen and nutrients in the outer retina in the macular region.

Combining the two scan regions together, the distribution of ChT in the posterior pole can be estimated, considering the continuity and integrity of the choroid in the macular and peripapillary regions. We can deduce that the ChT is thickest in the macular region and the area temporal and superior to the optic disc, followed by the area nasal to the optic disc, and is thinnest in the area inferior to the optic disc. To confirm the regional distribution of choroid, a wide-field ChT map focused on the posterior pole is required.

ChT According to Refractive Status

In the macular region, the choroid was thickest in hyperopes, followed by emmetropes, and was thinnest in myopes, which is similar to previous studies performed in both children and adults.[12,14,30] Similarly to a previous study,[14] our results suggest that the change in ChT is unevenly distributed; compared to

Table 4. Independent Factors Associated With ChTs in Different Regions

Variables	Unstandardized Coefficients B	Standardized Coefficients β	*t*-test	*P* Value	R^2
Macular region					
Central foveal ChT					0.325
Constant	541.507		5.702	<0.001	
SE	14.420	0.489	10.684	<0.001	
CR	−51.494	−0.203	−4.501	<0.001	
Central foveal RT	0.439	0.151	3.355	0.001	
UVA	22.896	0.137	3.008	0.003	
Parafoveal ChT					0.355
Constant	411.005		3.841	<0.001	
SE	11.193	0.416	8.839	<0.001	
Parafoveal RNFLT	−0.991	−0.185	−3.923	<0.001	
CR	−39.354	−0.170	−3.822	<0.001	
Parafoveal RT	0.525	0.129	2.652	0.008	
UVA	16.505	0.108	2.425	0.016	
Perifoveal ChT					0.318
Constant	268.928		2.609	0.009	
SE	8.010	0.355	6.303	<0.001	
CR	−25.514	−0.132	−2.750	0.006	
Perifoveal RT	0.742	0.202	3.566	<0.001	
Perifoveal RNFLT	−1.192	−0.153	−3.061	0.002	
UVA	12.096	0.095	2.049	0.041	
Peripapillary region					
Global PPCT					0.138
Constant	222.489		3.015	0.003	
Peripapillary RT	0.627	0.308	4.161	<0.001	
Peripapillary RNFLT	−1.180	−0.368	−5.228	<0.001	
SE	3.227	0.218	3.582	<0.001	
CR	−19.297	−0.152	−2.819	0.005	
Temporal PPCT					0.238
Constant	276.886		3.200	0.002	
SE	5.511	0.273	5.112	<0.001	
T2 RNFLT	−1.045	−0.316	−6.165	<0.001	
T2 RT	0.350	0.133	2.420	0.016	
CR	−19.373	−0.112	−2.254	0.025	
Superior PPCT					0.082
Constant	198.014		2.489	0.013	
S2 RNFLT	−0.964	−0.443	−5.015	<0.001	
S2 RT	0.667	0.360	4.029	<0.001	
CR	−17.375	−0.112	−2.085	0.038	
Inferior PPCT					0.147
Constant	266.064		3.721	<0.001	
SE	4.300	0.270	4.876	<0.001	
I2 RNFLT	−0.841	−0.442	−4.833	<0.001	
CR	−20.369	−0.149	−2.845	0.005	
I2 RT	0.388	0.234	2.427	0.016	
Nasal PPCT					0.099
Constant	259.101		3.633	<0.001	
N2 RNFLT	−0.751	−0.365	−5.529	<0.001	
N2 RT	0.299	0.181	2.725	0.007	
CR	−19.314	−0.123	−2.359	0.019	

T2, temporal sector of outer ring; N2, nasal sector of outer ring; I2, inferior sector of outer ring; S2, superior sector of outer ring.

hyperopes, choroidal thinning was most evident in the central foveal region, and was least evident in the perifoveal region in myopes. In the peripapillary region, we found that the choroid was thinner in myopes at the temporal and inferior sectors when comparing to the hyperopes, which were similar to a previous study,[22] while some studies have reported choroidal thinning at the nasal and superotemporal sectors in myopic children.[21,22] These disparities may be due to the difference in the instruments, protocols, and the refractive status of the participants. In our study, the most advanced OCT was used and the posterior border of the choroid was clearly detected. The mean thickness of choroid was calculated automatically and manual correction was made. Hence, our results are more accurate than those manual measurements. Moreover, children with different refractive status were included in our study, which can better reflect the real PPCT in the pediatric population.

Concerning the three myopic subgroups, no difference was observed between the moderate and high myopes in the macular region. This may be due to the relatively small sample size in these two subgroups and the small mean SE gap between these two subgroups. No differences in PPCT were

observed among the three myopic subgroups in the peripapillary region, which suggests that the worsening of myopia affect more of the choroid in the macular than the choroid in the peripapillary region in childhood. However, a study carried out in high myopic young adults showed that the PPCTs were thinner in all high myopic subgroups than those in the emmetropes, and the PPCTs became thinner as the degree of myopia increased in all sectors.[20] This suggests that with the worsening of myopia, the choroid in the peripapillary region may gradually be affected. Choroidal thinning in the peripapillary region may become evident in the early adulthood, but not childhood, in high myopes.

To conclude, our results suggest that there is an uneven myopia-related thinning of the choroid in the posterior pole. Thinning of the choroid in myopes may initially occur at the macular region and at the temporal and inferior sectors of the peripapillary region. Furthermore, choroidal thinning is most obvious in the area between the central fovea and optic disc, followed by other parts of the macular region and the temporal and inferior sectors of the peripapillary region, while the superior and the nasal sectors are least affected during the early development of myopia in childhood. However, with the increase in the degree of myopia and the prolonged course of myopia, the ChT in the superior region and nasal region may also be affected. To confirm this, longitudinal studies including different levels of myopia are needed.

Independent Factors of ChT Throughout the Posterior Pole

Our study showed that SE, UVA, CR, RT, and RNFLT (except for the central foveal region) were the independent factors of ChT in the macular region. Nonetheless, age and height were not significantly associated with ChT as independent factors in our study. In previous studies, there was a decreasing ChT with increasing age in Asian children and an increasing ChT with increasing age in white children in the central foveal region.[6–8,10–15] Moreover, one research with large sample size carried our by our study group showed that age was positively related to ChT in emmetropic and mild myopic (SE $>$ −2.00 D) children, while no relationship was found between age and ChT in children with SE $\leq$ −2.00 D.[16] Another our previous study also showed that the ChT was associated with height,[11] while height was not included in the model in this study. Different age distribution of the samples and different measurement methods of ChT may have contributed to these markedly different results. Similarly to previous studies,[12,14] we found a decreasing ChT in the macular region with the increase in the degree of myopia.

In the peripapillary region, SE was an independent factor of PPCT in the temporal and inferior sector, but not in the nasal and superior sector, which indicated an uneven change in PPCT during the development of myopia. This may suggest an uneven expansion of the fundus in the peripapillary region during the early stage of myopia, as expansion of the fundus may lead to choroidal thinning and atrophy. Additionally, some previous studies have found there to be a negative correlation between AL and PPCT either partially or globally,[20–22,28] while other studies reported that neither the SE nor the AL was independently associated with PPCT.[24,31] Relationship between SE and PPCT is more reliable in our study than previous results, as children with different refractive status and different degree of myopia were included in the study and the sample size was large. The relationship between age and PPCT is also disputed, as the current study and some previous studies showed no significant correlations,[20,22,26,31] while some other studies indicated a negative correlation between the two parameters.[24,28] The mean age of the participants may influence this relationship, as results from children and young adults showed no significant correlations.[20,22] As the age range is narrow in our study, researches with wider age range are needed in the future to confirm the relationship.

Limitations

The current study had several limitations that should be acknowledged. Firstly, the regionalization of the posterior pole was not based on Fovea-Bruch's membrane opening (BMO) centroid axis. In recent years, several studies have performed their regionalization along the Fovea-BMO axis and reported different results in RNFL thickness measurements when compared to the regionalization along the traditional horizontal axis.[32–36] It is better to acquire the images along the Fovea-BMO axis, as the disc fovea angle (the angle between the horizontal axis and the Fovea-BMO axis) may be different among individuals and the regionalization will be affected by the disc fovea angle. Limited by the OCT software, we performed regionalization along the horizontal axis, and tiny differences may exist between these two methods. To further display the potential difference, we measured the disc fovea angle on the 2D retinal image with Photoshop software. The mean disc fovea angle was (6.02 ± 2.98)° for the whole study population, and was (6.12 ± 2.77)°, (4.95 ± 3.52)°, and (6.46 ± 3.11)° for the myopic, emmetropic, and hyperopic group, respectively. The disc fovea angle was smaller in the emmetropic group than the myopic (P = 0.038) and the hyperopic group (P = 0.021), while no statistically significant difference was observed between the myopic and the hyperopic group. In spite of the statistically significant difference, the absolute difference was approximately 1° between the emmetropic group and the myopic or the hyperopic group, and the influence should be small. More studies are needed in the future to compare the differences between these two methods in ChT measurements. In addition, the BMO size was not measured in the current study and it may affect comparisons of ChT among different refractive groups. Further studies are needed to confirm the relationship between BMO size and ChT. Secondly, the number of children with high myopia was small, and the degree of myopia was not severe enough; hence, the ChTs of the moderate and high myopic subgroup in the macular region as well as the PPCTs of the three myopic subgroups were not significantly different. Thirdly, the current study has not included the preterm history information collection, which may be an independent factor of ChT. Fourthly, this was a cross-sectional study, and causal relationships between ChT and other parameters cannot be determined. Thus, long-term follow-up study will be necessary in the future. Last but not the least, this study was carried out in Chinese children aged between 9 and 16 years. The results from our study may not be applicable to children from other ethnicities and other age groups. Further studies including different races and age brackets should be performed to compensate for this limitation.

Conclusions

This study was the first to explore ChT in a wide area of the fundus in both the macular and peripapillary region in a large sample of Chinese children with varying degrees of refractive error. The change of ChT throughout the posterior pole with the development of myopia can be estimated from our study. As the choroid provides nutrients for the outer retina, thinning or atrophy of the choroid may lead to dysfunction or atrophy of the outer retina. From this point of view, chorioretinal atrophy

may occur first in the area between the central fovea and the optic disc, followed by the other parts of the macular region, the temporal and inferior sectors of the peripapillary region, while the superior and the nasal sectors of the peripapillary region are affected last. As thinning of the choroid may be the result of posterior pole expansion and posterior staphyloma formation, regional differences in choroidal thinning may also reflect an uneven expansion of the posterior pole during the development of myopia and predict the probability of developing posterior staphyloma. To confirm this speculation and to determine the sequence of changes in ChT, follow-up studies with larger sample sizes and wide-field ChT maps of the posterior pole will be needed in the future.

Acknowledgments

Supported by the National Natural Science Foundation of China for Young Staff (Grant No. 81402695), the Three-year Action Program of Shanghai Municipality for Strengthening the Construction of the Public Health System (2011–2013; Grant No. 2011-15, 2015-2017, and GWIV-13.2), the Key Discipline of Public Health–Eye Health in Shanghai (Grant No. 15GWZK0601), and the Overseas High-end Research Team–Eye Health in Shanghai (Grant No. GWTD2015S08). The sponsor or funding organization had no role in the design or conduct of this research.

Disclosure: **J. Deng**, None; **X. Li**, None; **J. Jin**, None; **B. Zhang**, None; **J. Zhu**, None; **H. Zou**, None; **X. Xu**, None; **J. Xie**, None; **L. Wang**, None; **S. Zhu**, None; **X. He**, None

References

1. Bill A, Sperber G, Ujiie K. Physiology of the choroidal vascular bed. *Int Ophthalmol*. 1983;6:101–107.
2. Parver LM. Temperature modulating action of choroidal blood flow. *Eye (Lond)*. 1991;5(pt 2):181–185.
3. Troilo D, Nickla DL, Wildsoet CF. Choroidal thickness changes during altered eye growth and refractive state in a primate. *Invest Ophthalmol Vis Sci*. 2000;41:1249–1258.
4. Spaide RF, Koizumi H, Pozzoni MC. Enhanced depth imaging spectral-domain optical coherence tomography. *Am J Ophthalmol*. 2008;146:496–500.
5. Ikuno Y, Kawaguchi K, Nouchi T, et al. Choroidal thickness in healthy Japanese subjects. *Invest Ophthalmol Vis Sci*. 2010; 51:2173–2176.
6. Li XQ, Jeppesen P, Larsen M, et al. Subfoveal choroidal thickness in 1323 children aged 11 to 12 years and association with puberty: the Copenhagen Child Cohort 2000 Eye Study. *Invest Ophthalmol Vis Sci*. 2014;55:550–555.
7. Park KA, Oh SY. Choroidal thickness in healthy children. *Retina*. 2013;33:1971–1976.
8. Nagasawa T, Mitamura Y, Katome T, et al. Macular choroidal thickness and volume in healthy pediatric individuals measured by swept-source optical coherence tomography. *Invest Ophthalmol Vis Sci*. 2013;54:7068–7074.
9. Read SA, Alonso-Caneiro D, Vincent SJ, et al. Longitudinal changes in choroidal thickness and eye growth in childhood. *Invest Ophthalmol Vis Sci*. 2015;56:3103–3112.
10. Ruiz-Moreno JM, Flores-Moreno I, Lugo F, et al. Macular choroidal thickness in normal pediatric population measured by swept-source optical coherence tomography. *Invest Ophthalmol Vis Sci*. 2013;54:353–359.
11. He X, Jin P, Zou H, et al. Choroidal thickness in healthy Chinese children aged 6 to 12: The Shanghai Children Eye Study. *Retina*. 2017;37:368–375.
12. Jin P, Zou H, Zhu J, et al. Choroidal and retinal thickness in children with different refractive status measured by swept-source optical coherence tomography. *Am J Ophthalmol*. 2016;168:164–176.
13. Zhang JM, Wu JF, Chen JH, et al. Macular choroidal thickness in children: The Shandong Children Eye Study. *Invest Ophthalmol Vis Sci*. 2015;56:7646–7652.
14. Read SA, Collins MJ, Vincent SJ, et al. Choroidal thickness in myopic and nonmyopic children assessed with enhanced depth imaging optical coherence tomography. *Invest Ophthalmol Vis Sci*. 2013;54:7578–7586.
15. Read SA, Collins MJ, Vincent SJ, et al. Choroidal thickness in childhood. *Invest Ophthalmol Vis Sci*. 2013;54:3586–3593.
16. Xiong S, He X, Deng J, et al. Choroidal thickness in 3001 Chinese children aged 6 to 19 years using swept-source OCT. *Sci Rep*. 2017;7:45059.
17. Margolis R, Spaide RF. A pilot study of enhanced depth imaging optical coherence tomography of the choroid in normal eyes. *Am J Ophthalmol*. 2009;147:811–815.
18. Wei WB, Xu L, Jonas JB, et al. Subfoveal choroidal thickness: the Beijing Eye Study. *Ophthalmology*. 2013;120:175–180.
19. Ding X, Li J, Zeng J, et al. Choroidal thickness in healthy Chinese subjects. *Invest Ophthalmol Vis Sci*. 2011;52:9555–9560.
20. Gupta P, Cheung CY, Saw SM, et al. Peripapillary choroidal thickness in young Asians with high myopia. *Invest Ophthalmol Vis Sci*. 2015;56:1475–1481.
21. Read SA, Alonso-Caneiro D, Vincent SJ, et al. Peripapillary choroidal thickness in childhood. *Exp Eye Res*. 2015;135: 164–173.
22. Wu XS, Shen LJ, Chen RR, et al. Peripapillary choroidal thickness in Chinese children using enhanced depth imaging optical coherence tomography. *Int J Ophthalmol*. 2016;9: 1451–1456.
23. Tan CS, Ouyang Y, Ruiz H, et al. Diurnal variation of choroidal thickness in normal, healthy subjects measured by spectral domain optical coherence tomography. *Invest Ophthalmol Vis Sci*. 2012;53:261–266.
24. Huang W, Wang W, Zhou M, et al. Peripapillary choroidal thickness in healthy Chinese subjects. *BMC Ophthalmol*. 2013;13:23.
25. Tanabe H, Ito Y, Terasaki H. Choroid is thinner in inferior region of optic disks of normal eyes. *Retina*. 2012;32:134–139.
26. Ho J, Branchini L, Regatieri C, et al. Analysis of normal peripapillary choroidal thickness via spectral domain optical coherence tomography. *Ophthalmology*. 2011;118:2001–2007.
27. Schoenwolf G, Bleyl S, Brauer P, et al. *Larsen's Human Embryology*. Philadelphia: Elsevier; 2009:602–616.
28. Jiang R, Wang YX, Wei WB, et al. Peripapillary choroidal thickness in adult Chinese: The Beijing Eye Study. *Invest Ophthalmol Vis Sci*. 2015;56:4045–4052.
29. Oh J, Yoo C, Yun CM, et al. Simplified method to measure the peripapillary choroidal thickness using three-dimensional optical coherence tomography. *Korean J Ophthalmol*. 2013; 27:172–177.
30. Esmaeelpour M, Povazay B, Hermann B, et al. Three-dimensional 1060-nm OCT: choroidal thickness maps in normal subjects and improved posterior segment visualization in cataract patients. *Invest Ophthalmol Vis Sci*. 2010;51: 5260–5266.
31. Erbagci H, Oren B, Okumus S, et al. Peripapillary choroidal thickness in healthy Turkish subjects. *Clin Ophthalmol*. 2015; 9:1393–1397.
32. Araie M, Iwase A, Sugiyama K, et al. Determinants and characteristics of Bruch's membrane opening and Bruch's

membrane opening-minimum rim width in a normal Japanese population. *Invest Ophthalmol Vis Sci*. 2017;58:4106–4113.

33. Chauhan BC, Danthurebandara VM, Sharpe GP, et al. Bruch's membrane opening minimum rim width and retinal nerve fiber layer thickness in a normal white population: a multicenter study. *Ophthalmology*. 2015;122:1786–1794.
34. Chauhan BC, Burgoyne CF. From clinical examination of the optic disc to clinical assessment of the optic nerve head: a paradigm change. *Am J Ophthalmol*. 2013;156:218–227.
35. Garway-Heath DF, Poinoosawmy D, Fitzke FW, et al. Mapping the visual field to the optic disc in normal tension glaucoma eyes. *Ophthalmology*. 2000;107:1809–1815.
36. Valverde-Megias A, Martinez-de-la-Casa JM, Serrador-Garcia M, et al. Clinical relevance of foveal location on retinal nerve fiber layer thickness using the new FoDi software in spectralis optical coherence tomography. *Invest Ophthalmol Vis Sci*. 2013;54:5771–5776.

Investigative Ophthalmology & Visual Science